Norwegian Meteorological Institute
met.no

met.no report

**Report no. 1/2013**
**Oceanography**
**ISSN: 1503-8025**
**Oslo, February 22, 2013**

# BaSIC Technical Report No. 1
# The triply nested model system

**Lars Petter Røed and Nils Melsom Kristensen**

**With contributions from**
**Jon Albretsen and Bjørn Ådlandsvik[1]**

**Contract No. 4502465983**

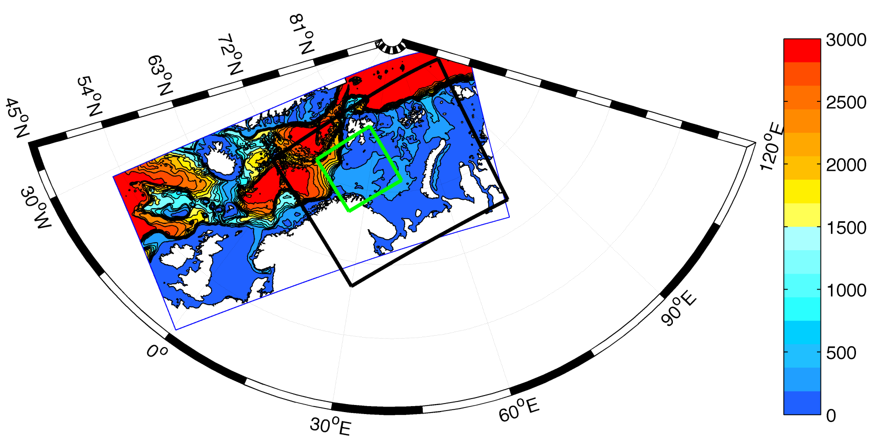


INSTITUTE OF MARINE RESEARCH
HAVFORSKNINGSINSTITUTTET

Norwegian
Meteorological Institute
met.no

[1]Lars Petter Røed and Nils Melsom Kristensen are affiliated with the Norwegian Meteorological Institute (met.no), Oslo, Norway. Jon Albretsen and Bjørn Ådlandsvik are affiliated with Institute of Marine Research (IMR), Bergen, Norway. Lars Petter Røed is also affiliated with the Department of Geosciences, Section Meteorology and Oceanography, University of Oslo, Norway

Norwegian
Meteorological Institute
met.no

**report**

| Number | Subject | Date | Classification | ISSN |
|---|---|---|---|---|
| 1/2013 | Oceanography | February 22, 2013 | ☒ Open<br>☐ Restricted<br>☐ Confidential | 1503-8025 |

**Title**

BaSIC Technical Report No. 1
The triply nested model system

**Authors**

Lars Petter Røed and Nils Melsom Kristensen

| Client(s) | Client reference |
|---|---|
| Statoil (Børge Kvingedal) | Contract No. 4502465983 |

**Abstract**

Described is the present version (as of February 21, 2013) of the triply nested model system that we are presently developing as part of the BaSIC (Barents Sea Ice and Currents) project. It consistes of the SVIM 4 km mesh model, the BaSIC 2 km mesh model and the BaSIC 800 m mesh model. In addition to describing the technical set-up of the BaSIC system we also discuss the results from a 150 day test hindcast starting January 1, 2000. The results encourage us to do more work regarding open boundary conditions (nesting techniques). Furthermore, we recommend to consider using sea surface salinity and sea ice nudging in all three models, and consider enlarging the computational domain of the intermediate BaSIC 2 km mesh model.

**Keywords**

Physical Oceanography, Numerical Modeling, Barents Sea, Sea-ice, Circulation

| Disiplinary signature | Responsible signature |
|---|---|
| Lars Anders Breivik, Head Section Ocean and Ice | Øystein Hov, Head Research and Development Department |

**Postal address** PO Box 43 Blindern N-0313 Oslo Norway
**Office** Niels Henrik Abels vei 40
**Telephone** +47 2296 3000
**Telefax** +47 2296 3050
**e-mail:** met.inst@met.no **Web:** met.no
**Bank account** 7694 05 00601
**Swift code** DNBANOKK

# Contents

# List of Tables

# List of Figures

# List of abbrevations

Abbreviation used in the text.

- BaSIC = Barents Sea Ice and Currents
- SVIM = Spatiotemporal Variability In Mortality and growth of fish larvae and zooplankton in the Lofoten-Barents Sea ecosystem
- IMR = Institute of Marine Research, Norway
- met.no = Norwegian Meteorological Institute, Oslo, Norway
- NIVA = Norwegian Institute of Water Research, Oslo, Norway
- ROMS = Regional Ocean Modeling System

# 1 Purpose and scope

## 1.1 Background

To prepare for eventual oil and gas exploration in the Kara and Barents Seas it is of general importance to get a good understanding of the environment. In particular, it is of interest to get knowledge of the meteorological and oceanographic variables such as winds, waves, water level (tidal height and storm surge), currents and ice conditions to design offshore structures that are both safe and cost efficient. This requires sufficiently accurate information about long-term cycles and trends of these variables. To this end long term records, say 20 to 40 years duration, are needed. A cost efficient means by which such time series can be provided is by performing long term hindcasts using numerical models. Such long time series have recently been established for atmospheric variables and waves through an earlier joint industry project (JIP) (*Reistad et al.*, 2009, 2011). In the project BaSIC the aim is to establish corresponding long term time series regarding sea ice, currents, water level and hydrography (temperature and salinity).

Record length is less of an issue for currents than it is for wind and waves because currents have less significant year to year variations. On the other hand, currents have more significant place to place variations than wind and waves. Numerical circulation models of sufficient grid resolution can describe this variability. Current hindcasts generated by such suitable models yield estimates of extreme values for design of facilities, operating conditions, and local variations of currents. Modeled currents also inform measurement campaign strategy.

There is strong inter-annual and inter-decadal climatic variability in the Barents Sea region (*Kvingedal*, 2005). In order to understand this variability, hindcasts of at least 25 years duration are needed. Ice occurs in most parts of the Barents Sea region. Currents are one of the biggest forces that move ice. High quality current data for the entire region are essential for the design of structures that can withstand icebergs, sea ice, and ice ridges. Operability and collision risk analyses must include modeled current data.

To meet these needs, and in particular to get knowledge of the place to place variation of currents, we proposed, within the project BaSIC, to develope a triply nested model system based on the experience we have gained in developing such a system to meet the need for sufficiently high resolution current forecasts along the Norwegian coast. If successful we later embark on producing the long term hindcast to provide the necessary long term records. This report describes the development of the triply nested system as of February 21, 2013.

## 1.2 The NOWP system at the Norwegian Meteorological Institute

The BaSIC model system is based on the recently developed triply nested operational numerical ocean weather prediction (NOWP) system at the Norwegian Meteorological Institute (met.no). It is thus based on the regional ocean modeling system ROMS (*Haidvogel et al.*, 2008; *Shchepetkin and McWilliams*, 2005). A recent forecast produced by the triply nested NOWP system is depicted in Figure 1 showing the 24 hour average current speed at 3 m depth valid for February 23, 2013. The outermost model in the triply nested NOWP system is the Arctic 20 km mesh model (A20). It is forced by the UK Met Office global ocean model FOAM

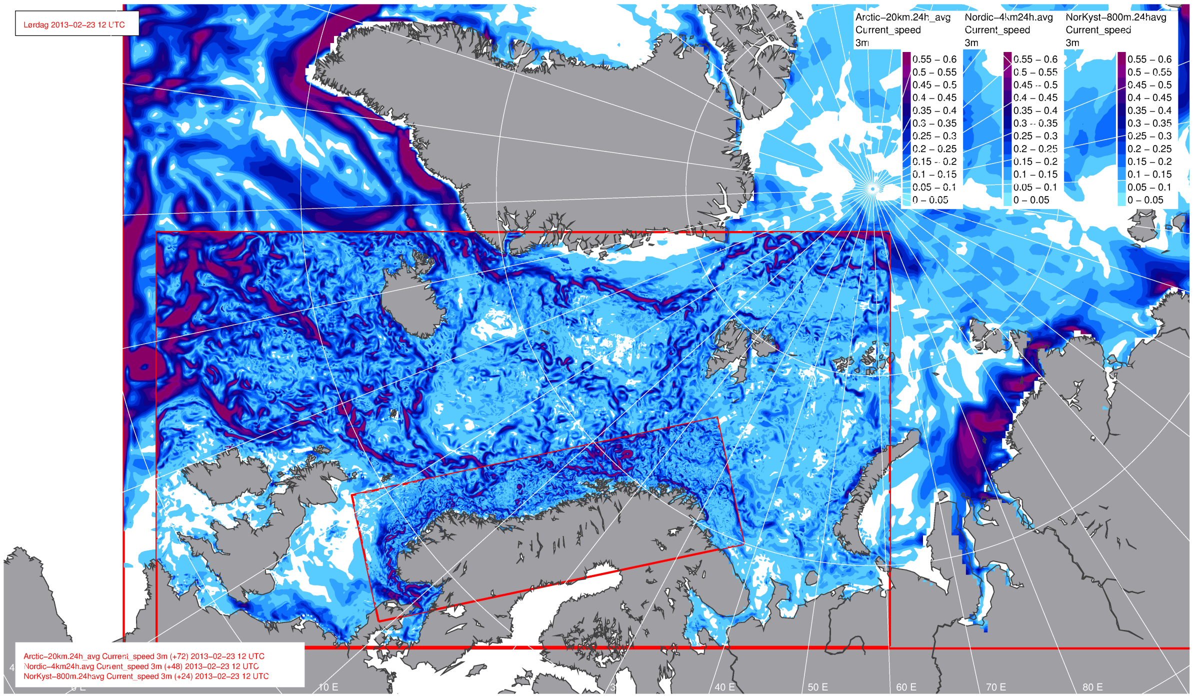


Figure 1: Displayed is the the 24 hour average current speed at 3 m depth for the Nordic Seas and the Arctic Ocean and adjacent seas on February 23, 2013. The picture is extracted from the recently established triply nested NOWP system at met.no. The outermost model is the Arctic 20 km mesh model covering the Arctic Ocean, the Atlantic Ocean north of 50$^o$N (only a subdomain is shown here). The intermediate model is the Nordic 4 km mesh model covering the Nordic Seas and the adjacent Barents and North Seas. Finally the innermost model is an 800 m mesh model covering basically the Norwegian coast from teh Swedish to the Russian border. The color scale gives the speed in intervals of 0.05 m/s in the range 0 to 0.6 m/s. Note the increased fin mesh patterns emerging when increasing the resolution.

on its lateral boundary to the south. Into A20 is nested the Nordic 4 km mesh model (N4). Finally an 800 m mesh model (henceforth N800) is nested into N4.

The N800 model is based on the NorKyst-800 model (*Albretsen et al.*, 2011), which was developed as a collaborative effort by and between met.no, the Institute of Marine Research (IMR) and the Norwegian Institute of Water Research (NIVA). As shown in Figure 2, showing the 24 average sea surface current (SSC) and sea surface temperature (SST) valid for February 15, 2013, the N800 model covers the Norwegian Shelf areas only. As of January 1, 2013 the triply nested NOWP system based on ROMS is the one and only provider of all national ocean forecasts disseminated by met.no. Figures 1 and 2 nicely indicate the gain obtained in place to place variations in currents and temeprature when the mesh size is decreased (increased resolution).

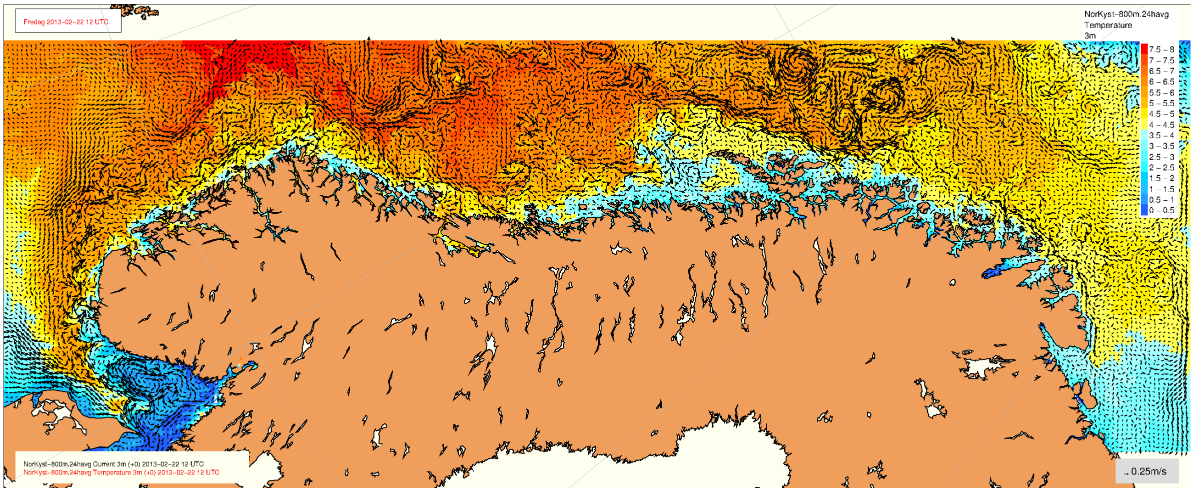


Figure 2: Displayed is the forecast of the the 24 hour average currents (arrows) and temperature (colors) at 3 m depth valid for February 22, 2013. It is extracted from the operational triply nested NOWP system at met.no. The color scale has a contour interval of 0.5$^o$C in the range from 0 to 8$^o$C. The currents are shown as arrows with the length of the arrow giving the strength of the currents. Only every tenth arrow is plotted. A strength of 0.25 m/s is shown in the lower right-hand corner.

### 1.3 Report organization

In developing the triply nested system for the BaSIC project we take advantage of the work done in developing the ROMS NOWP system. In the following we present the models making up the triply nested BaSIC system, their configuration and technical characteristics (Sections 2 and 3). In Section 4 we present some results in terms of 30 day averages of sea surface currents (SSC), sea surface temperature (SST), sea surface salinity (SSS) and sea surface relative velocity ($\omega$) from the BaSIC 2 km mesh model and the SVIM 4 km mesh model. Conclusions and recommendations are finally presented in Section 5.

## 2 Configuration of the triply nested BaSIC model system

### 2.1 Computational domains and model topographies

The triply nested BaSIC model system, as the name indicates, consists of three models. They cover three different geographical areas as shown in Fig. 3, and are nested into each other. The outermost model, for which also the bottom topography is plotted, is the SVIM 4 km mesh model. It covers the Nordic Seas including the adjacent Barents and North Seas. The area bounded within the black lines conforms to the BaSIC 2 km mesh model covering the Barents and Kara Seas. It also includes waters west and north of the Svalbard Archipelago and Franz Josef Land. The innermost model, whose area is bounded by the green lines in Figure 3, conforms to the area covered by the BaSIC 800 m mesh model, and stretches from Nordkapp to the tip of Spitsbergen.

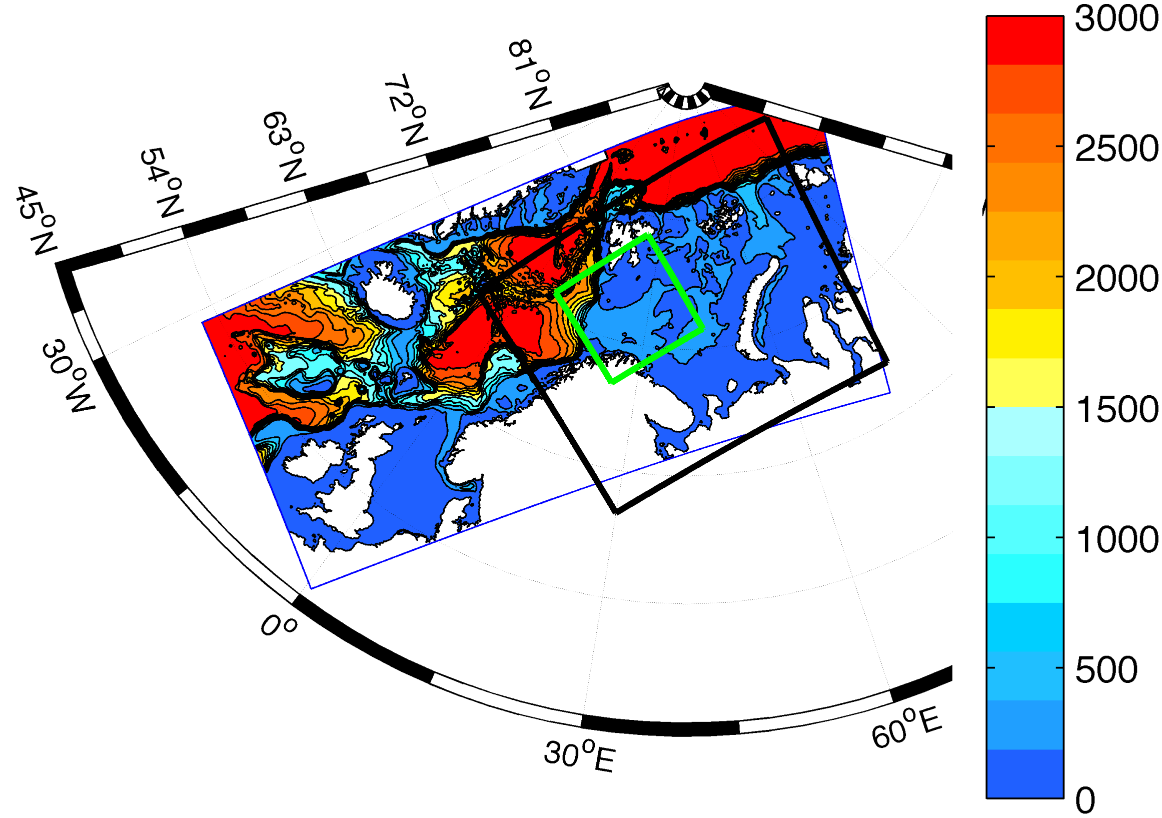


Figure 3: Outlined is the geographical coverage of the three models included in the triply neste BaSIC model system currently developed for the BaSIC project. The innermost model outlined by the green rectangle is the area covered by the BaSIC 800 m mesh model. The domain outlined by the black rectangle is the area covered by the BaSIC 2 km mesh model, while the outermost domain is the area covered by the SVIM 4 km mesh model. Only the topography of the SVIM 4 km mesh model is shown. The color scale indicates the depth in intervals of 187.5 m and in the range 0 to 3000 m.

The topography of the SVIM 4 km mesh model, the BaSIC 2 km mesh model, and the BaSIC 800 m mesh model are shown in Figures 4 and 5 to better appreciate differences in their respective topographies. Note that the topography shown in Figure 4 for the SVIM 4 km mesh model is a subdomain in conformance with the area plotted for the BaSIC 2 km mesh model. Similarly is the topography shown in Figure 5 for the BaSIC 2 km mesh model a subdomain. As expected we note that the only differences between the topographies are associated with finer and finer structures as we increase the resolution (decreases the mesh size). The larger scale patterns remain the same.

The major topographic features of the BaSIC 2 km mesh model's area are the Mid-Atlantic Ridge, the steep shelf slope in the Lofoten area continuing northward toward the Arctic Ocean, the Yermak Plateu north of Svalbard and the shelf slope north of Svalbard and Franz Josef Land. Worth mentioning is also the canyon east of Franz Josef land, and the various banks in the Barents Sea.

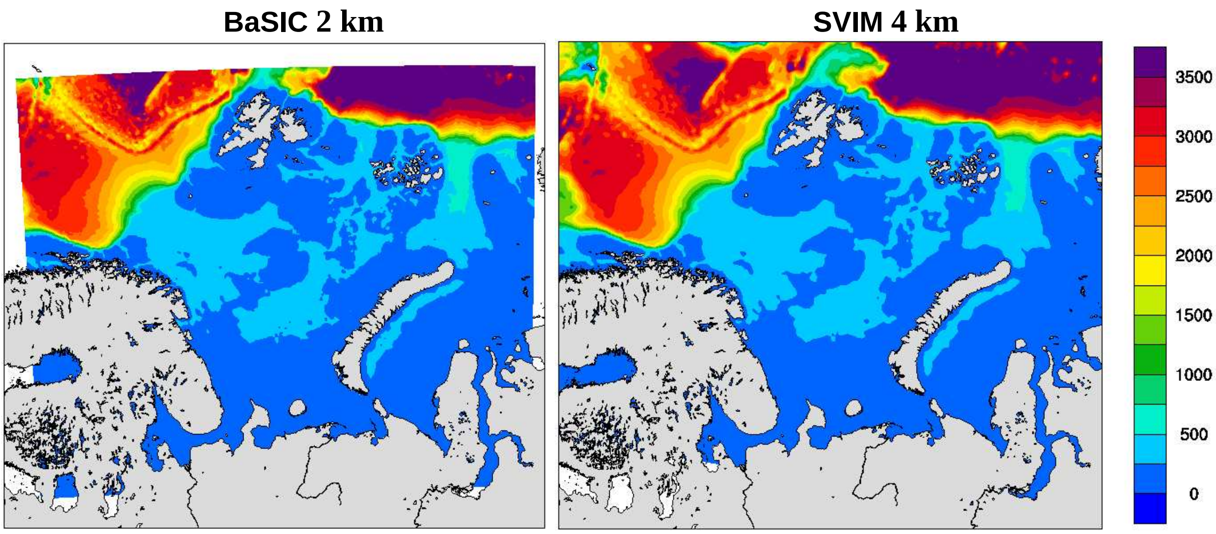


Figure 4: Displayed is the bottom topography of the BaSIC 2 km mesh model (left-hand panel) and the SVIM 4 km mesh model (right-hand panel). Colors indicate depth in meters in intervals of 250 m in the range 0 to 3500 m. Note the differences in the fine structures.

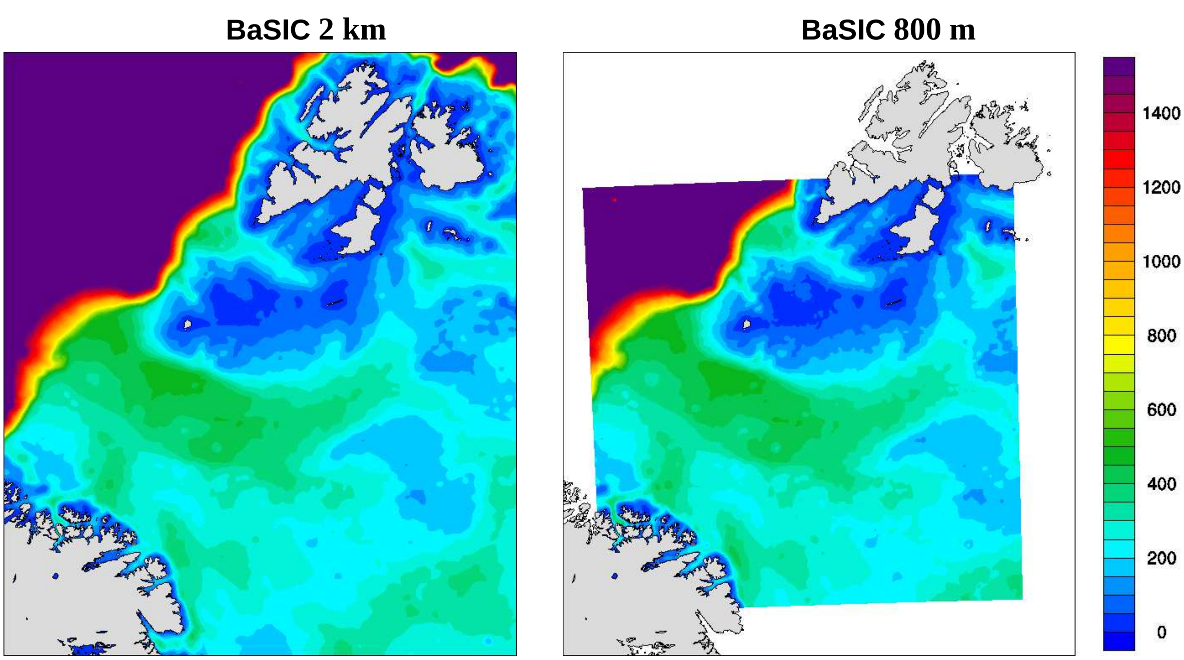


Figure 5: Displayed is the bottom topography of the BaSIC 2 km mesh model (left-hand panel) and the BaSIC 800 m mesh model (right-hand panel). Colors indicate depth in meters in intervals of 50 m and in the range 0 to 1500 m. Note the differences in the fine structures.

## 2.2 Model set up

### 2.2.1 Mesh sizes

When discussing mesh sizes we emphasize that we often us the phrase eddy resolving, eddy permitting and non-eddy resolving models. These phrases are related to the so called Rossby radius of deformation. For instance the phrase eddy resolving is used to acknowledge that the model properly resolves the Rossby radius, that is, that the model is able to resolve the processes that generates mesoscale features such as current jet filaments, meanders and eddies. Commonly this require that the ratio between the Rossby radius and the distance between grid points (grid resolution) is about 4-10. An eddy permitting model is a model which are able to sustain eddies once formed. This requires a ratio of about 1. A non-eddy resolving model is one in which the ratio of the Rossby radius and the grid resolution is smaller than 1.

The Rossby deformation radius in the Barents Sea area is about 4-5 km. The SVIM 4 km mesh model is hence only eddy permitting, while the BaSIC 2 km mesh model with a mean grid reolution of 2 km is bordering on being eddy resolving with a ratio of about 2-3. The only truly eddy resolving model of the three is the BaSIC 800 m mesh model. For this model the ratio is about 5-6.

### 2.2.2 Atmospheric forcing

The atmospheric variables necessary to derive momentum, heat and freshwater fluxes at the surface are extracted from the ERA-Interim reanalysis project (*Dee et al.*, 2011). These fields have a spatial resolution of 0.25 degrees, but for the actual trial hindcast and hindcast, we intend to use the NORA10[2] (*Reistad et al.*, 2009, 2011) hindcast archive merged into ERA-Interim fields. The atmospheric variables extracted and made available to the ROMS model are the two lateral wind components at 10 meter height, the mean sea level pressure, the temperature at 2 meter height, the specific humidity at 2 meter height, the total cloud cover (in %) and the precipitation rate (must be specified as kg/m$^2$s). The atmospheric forcing fields has a temporal resolution of 6 hours, except for rainrates, which has a temporal resolution of 12 hours.

### 2.2.3 Lateral boundary forcing

The lateral boundary forcing to the BaSIC 2 km mesh model is provided by fields from the SVIM hindcast project consisting of daily mean currents, water level, temperature, salinity and ice variables. The SVIM hindcast project was run using ROMS on an extended domain compared to the operational Nordic 4 km model (Fig 1). Whereas the operational Nordic 4 km model stops at 60°E, the SVIM 4 km mesh model covers the Barents and Kara Seas to 80°E (Fig. 3). At the lateral open boundaries to the south, west and north the SVIM 4 km mesh model is forced by data from the SODA[3] reanalysis project.

[2] NORA10 is a dynamical downscaling of ERA using Hirlam 10km.

[3] Simple Ocean Data Assimilation

# 3 Characteristics of the models

The triply nested BaSIC model system is based on the model ROMS (Regional Ocean Modeling System). The canonical version of the latter is described in some detail in *Haidvogel et al.* (2008) and in *Shchepetkin and McWilliams* (2005). Here we focus on what is new and on the characteristics of the set up for the BaSIC project.

We use version 3.5 of ROMS of the so called ”Kate branch”. The main reason for using this branch is the coupling to a sea-ice model. The mesh sizes and number of vertical levels are given in Table 1. The BaSIC 2 km trial simulations was conducted on the supercomputer Vilje in Trondheim. The BaSIC 800 m simulations will be carried out on the Hexagon supercomputer in Bergen.

Table 1: Model facts

| Text | Unit | BaSIC 2 km | BaSIC 800 m |
|---|---|---|---|
| Mesh size | km | 2 | 0.8 |
| No. of vertical levels/layers | - | 35 | 35 |
| Horizontal dissipation | - | No explicit diffusion[1] | No explicit diffusion[1] |
| Vertical mixing | - | GLS mixing scheme[2] | GLS mixing scheme[2] |
| Mode splitting | - | yes | yes |
| Horizontal advection scheme | - | 3rd order upwind | 3rd order upwind |
| Long (internal) time step | s | 60 | 45 |
| Ratio of internal to external time step | - | 60 | 15 |

[1]There is some weak horizontal diffusion due to the application of the third order upwind advection scheme,
[2]*Umlauf and Burchard* (2003)

## 3.1 Vertical coordinate

We note that ROMS utilizes a generalized terrain-following vertical coordinate. Terrain-following implies that the vertical levels follow the bottom contours and transform the depth coordinate from a depth coordinate to a non-dimensional vertical coordinate, in ROMS denoted $s$, which has the range $s \in [-1, 0]$ with $s = 0$ at the surface and $s = -1$ at the bottom. For a detailed description of vertical coordinate system in ROMS we refer to *Song and Haidvogel* (1994) and *Shchepetkin and McWilliams* (2009). For a general description we refer to *Griffies* (2004, Chapter 6). The advantage of the generalization is that it allows us to simultaneously maintaining high resolution in the surface layer in deep water as well as dealing with steep and/or tall topography. This is crucial in our case because of the steep slopes encountered in the area, e.g., the shelf slopes off Lofoten continuing northward to Svalbard, and the Yermak plateu north of Svalbard (Figure 4). Depth of the *s* levels can be calculated using the *s*-coordinate formula of *Shchepetkin and McWilliams* (2009). In the BaSIC application we use $\theta_s = 6$, $\theta_b = 0.1$ and $hc = 30$, with Vtransform=2 and Vstretching=1. At a depth of 1000 meters these values gives levels at (from bottom and up) 927, 800, 693, 602, 525, 460, 405, 358, 318, 284, 254, 227, 203, 181, 161, 142, 123, 106, 90, 76, 63, 52, 43, 35, 29, 24, 19, 16, 13, 10, 8, 6, 4, 2 and 1 meters, respectively for the density levels.

## 3.2 Advection scheme

ROMS has a wide variety of advection schemes of relative high order. Here we use a 3rd order upwind biased scheme for the horizontal advection of momentum, salinity and temperature (*Shchepetkin and McWilliams*, 1998). In our experience this scheme has good properties in maintaining fronts and permitting mesoscale eddies and filaments. In the vertical the 4th order centered representation of *Haidvogel et al.* (2008) is used.

ROMS also offers several vertical mixing schemes. The one used here is the Mellor-Yamada 2.5 scheme of the Generic Length Scale (GLS) formulation of *Umlauf and Burchard* (2003). The implementation of this scheme in ROMS is documented in *Warner et al.* (2005). As displayed in Table 1 we emphasize that although no explicit horizontal diffusion is employed in ROMS, the 3rd order upwind scheme provides some implicit diffusion. The vertical diffusion is embedded in the GLS scheme.

## 3.3 Lateral forcing and open boundary conditions

All the models have open boundaries, at which lateral open boundary conditions are imposed. The SVIM 4 km mesh model, or grandparent model, was run as part of the project SVIM and provides conditions in terms of three-dimensional daily means of the two lateral components of current, temperature and salinity, and two-dimensional daily means of the two lateral components of the depth integrated (barotropic) current, ice concentration, ice thickness, snow thickness and sea surface elevation (water level). This information is extracted from the grandparent once per day. The information we extract is available at 0, 5, 10, 20, 30, 50, 75, 100, 150, 200, 250, 300, 400, 500, 600, 800, 1000, 1500, 2000 and 3000 m depth. Tidal elevation and tidal currents are specified separately (Section 3.5).

A variety of open boundary conditions are available in ROMS. In the present BaSIC system we use the recommended Chapman/Flather combination for the free surface and the two-dimensional variables. For the three-dimensional variables we use a radiation condition and nudging as described in *Marchesiello et al.* (2001) and *Albretsen et al.* (2011). It should be emphasized that *Mason et al.* (2010) reports that for long term integrations these open boundary or nesting conditions give rise to false boundary currents, so called rim currents. They also report in detail on how to modify the present conditions so as to minimize these false rim currents. It should be emphasized though that any fine scale motion created in the child model cannot be given to the parent model using a one-way nesting condition, and thus false currents at the boundaries of the child can never be avoided completely. In particular this is true at downstream boundaries (outgoing flow).

For river locations and discharges we use data from the EHYPE hydrological model. The river outlets are located as close as possible to their real position in the model grid, which sometimes are at the bottom of some of the fjords that cut inland from the main shoreline. We specify the rivers as a volume flux across the land-sea boundary approximately. A vertical profile is used, generally giving highest flow near the surface.

### 3.4 Atmospheric forcing and bottom friction

To convert atmospheric values to a momentum and heat flux input to the model the "Kate branch" replaces the standard ROMS bulk flux routine by the routines outlined in *Røed and Debernard* (2004) (*Albretsen et al.*, 2011). The bottom friction is quadratic and follows the formulation of *Gerritsen and Bijlsma* (1988), that is,

$$\tau_b = C|\mathbf{u}_b|^2\mathbf{u}_b \tag{1}$$

where $\tau_b$ is the bottom stress, $\mathbf{u}$ is the bottom velocity and $C$ is a constant dependent on the equilibrium depth (decreases with increasing equilibrium depth). The coefficient we use is $3.0 \cdot 10^{-3}$.

### 3.5 Tidal forcing

Both tidal elevation and depth integrated current is included in the boundary forcing by the aforementioned Chapman/Flather boundary condition which is designed for this purpose. Tidal information is extracted from the TPXO tidal data base. We extract eight constituents as outlined in *Albretsen et al.* (2011), namely the $M_2$, $K_1$, $K_2$, $N_2$, $S_2$, $P_1$, $O_1$, and $Q_1$ constituents.

### 3.6 Time stepping

To speed up the integration we use the mode splitting technique that comes with ROMS to separate the barotropic and baroclinic modes. It is a fairly advanced and recently developed scheme in particular regarding the exchange of information between the modes (*Shchepetkin and McWilliams*, 2005; *Haidvogel et al.*, 2008). The actual time step we use is 60 seconds for the baroclinic mode, and a ratio of 60 between the baroclinic and the shorter barotropic time step (cf. Table 1).

## 4 Results

To test the triply nested system we have performed a 150 day long test hindcast starting January 1, 2000. The results are presented as 30 day means covering the period April 29 - May 28, 2000, the last 30 days of the test hindcast. Below we present and briefly discuss the results.

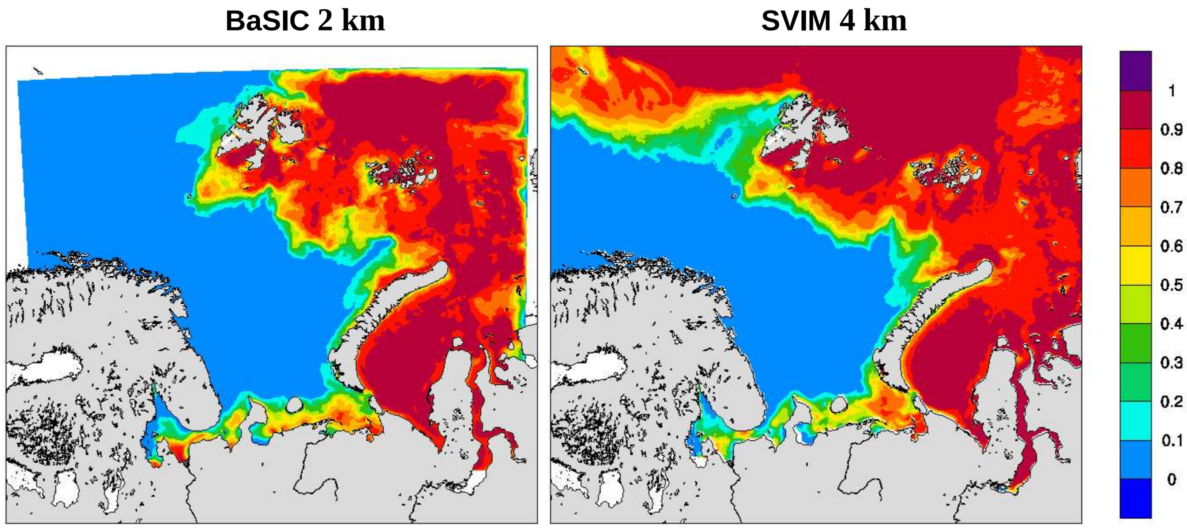


Figure 6: Displayed is the mean sea ice fraction for the 30 day period April 29 - May 28, 2000. The BaSIC 2 km mesh model to the left and the SVIM 4 km mesh model to the right. Colors indicate sea ice fraction in intervals of 0.1 in the range 0 to 1. Note the missing ice north of Jan Mayen towards Spitsbergen in the BaSIC 2 km mesh model.

## 4.1 Sea ice

We start with showing the sea ice fraction as displayed in Figure 6, that is, a fraction of 1 entails 100% ice cover. We immediately notice the lack of sea ice in the western part of the basin north of Jan Mayen towards Svalbard in the BaSIC 2 km mesh model. This due to the fact that no information about the sea ice that is depicted in the SVIM 4 km mesh model results (cf. the right-hand panel of Figure 6) is conveyed to the BaSIC 2 km mesh model. This minor glitch of major consequences is rectified in runs performed at present.

Furthermore, as expected, we observe that the small scale structures are enhanced in the BaSIC 2 km mesh model compared to the SVIM 4 km mesh model due to the higher resolution. We note that the larger scale picture is very much alike though, except in the area west and south of Spitsbergen where there is a lack of sea ice input along the lateral boundary.

## 4.2 Currents

Figure 7 shows the sea surface current (SSC) vectors ($\mathbf{u}_s$) as produced by the two models. It is interesting to note that the current patterns are almost identical, but that the currents in the BaSIC 2 km mesh model are definitely swifter than in the SVIM 4 km mesh model. Other noteable differences are the stronger and more abundant number of eddies in the BaSIC 2 km mesh model. In particular we notice the eddies off the Lofoten Archipelago. The latter is in line with those found earlier in the LOVECUR project (*Røed and Kristensen*, 2010, 2013). They are well known from observations (*Koszalka and LaCasce*, 2010; *Koszalka et al.*, 2011) as well as other numerical modeling studies (e.g., *Köhl*, 2007). Finally we note the presence of false currents at the boundaries between the BaSIC 2 km mesh model and the SVIM 4 km

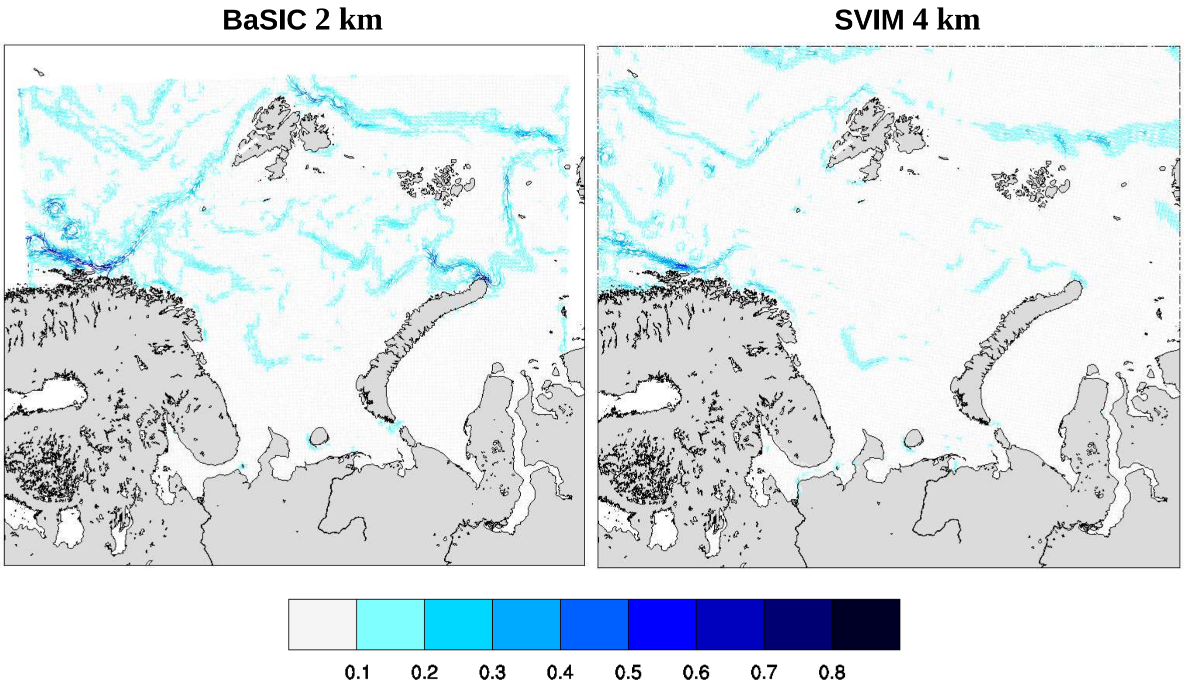


Figure 7: As Figure 6, but for the sea surface currents (SSC). Color scale indicate current speed in intervals of 0.1 m/s and in the range 0 to 0.8 m/s. Note the similarities in patterns, but that the speed are higher in the BaSIC 2 km mesh model. Also more eddies are appearent in the BaSIC 2 km mesh model, in particular in the Lofoten Basin.

mesh model, so called rim currents (e.g., *Mason et al.*, 2010). These are more enhanced and more visible when plotting the relative vorticity, that is, $\omega = \mathbf{k} \cdot \nabla \times \mathbf{u}_s$ as shown in Figure 8. Plotting $\omega$ also nicely enhances jet current filaments and eddies. For instance we immediately notice that the current jet filament extending northward towards Spitsbergen from the Lofoten area, and that the jet is directed northwards. Furthermore, we recognize the filament north of Svalbard as being directed eastward. Also enhanced when plotting the relative vorticity are eddies. A nice example are the eddies off Lofoten that stand out as green to blue dots signaling that they are anticyclones ($\omega < 0$). These observations are of course in accordance with the SSCs shown in Figure 7.

## 4.3 Water level

The results in terms of the water level height (SSH) is shown in Figure 9. Note that due to the 30 day averaging there is no tides left in the SSH shown. We immediately observe that the SSH is much higher in the shallow water areas along the Norwegian coast from the Lofoten-Vesterålen area and northwards along the Norwegian coast and further continuing along the Russian coast in the BaSIC 2 km mesh model than in the SVIM 4 km mesh model. The gradients in the SSH is therefore stronger in the BaSIC 2 km mesh model than in the SVIM 4 km mesh model. This enhances the depth integrated current component in the BaSIC 2 km

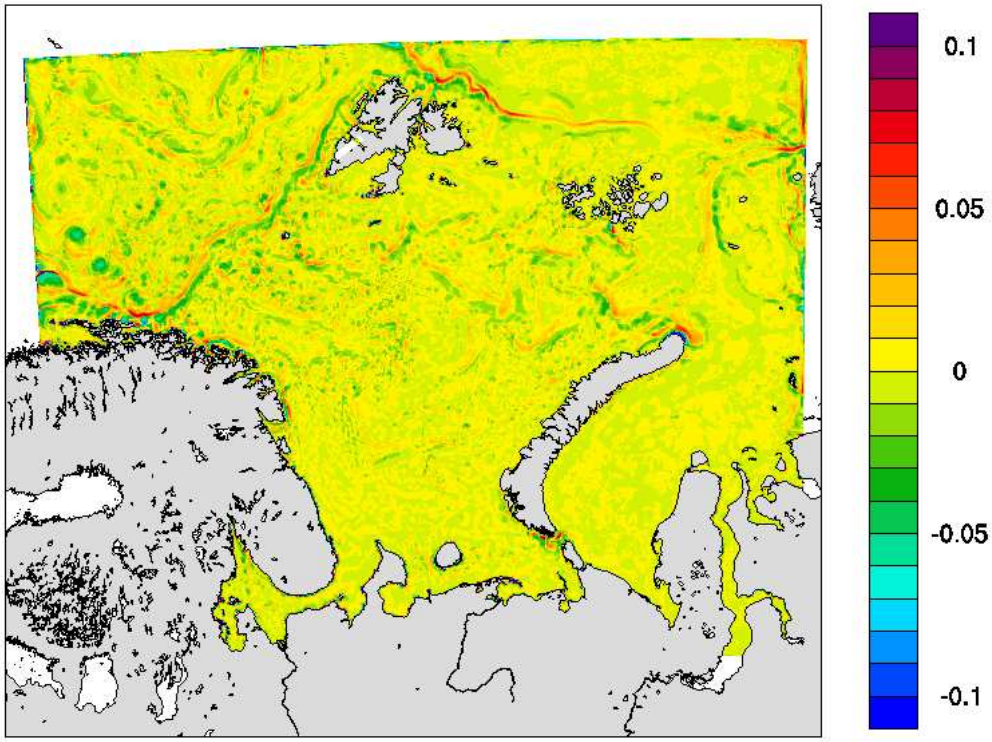


Figure 8: As Figure 6, but for the relative vorticity and only showing the results from the BaSIC 2 km mesh model. Note the appearance of the anomalies along the open boundaries indicating false currents at the boundaries often referred to as rim currents. Negative values indicate anticyclones (high pressure systems) while positive values indicate cyclones (low pressure systems). Color scale gives relative vorticity in $10^{-3}s^{-1}$ in intervals of $0.01{\cdot}10^{-3}s^{-1}$.

mesh model, corroborated by the SSCs displayed in Figure 7, which indeed shows stronger and swifter currents in the BaSIC 2 km mesh model than in the SVIM 4 km mesh model. Finally it is interesting to note that the eddies off Lofoten also stand out in the SSH picture. The eddies are hence almost barotropic and therefore reaching deep down into the water column.

## 4.4 Temperature and salinity

The associated hydrographic fields in terms of the 30 day mean of the sea surface temperature (SST) and the sea surface salinity (SSS) are displayed in Figures 10 and 11, respectively. Regarding the SST the main difference between the two models is the warmer coastal water and the appearent advection of more warm water northward toward Spitsbergen. This is obviously associated with the enhanced current jets in the BaSIC 2 km mesh model compared to the SVIM 4 km mesh model (Fig. 7) due to the enhanced gradients in the water level (Fig. 9).

There are also large differences in the SSS for the two models (Fig. 11). Most prominent are the enhanced SSS values in the Lofoten Basin and the enhanced SSS values in the Kara Sea. Furthermore there are some curious high SSS values along the Russian coast east of

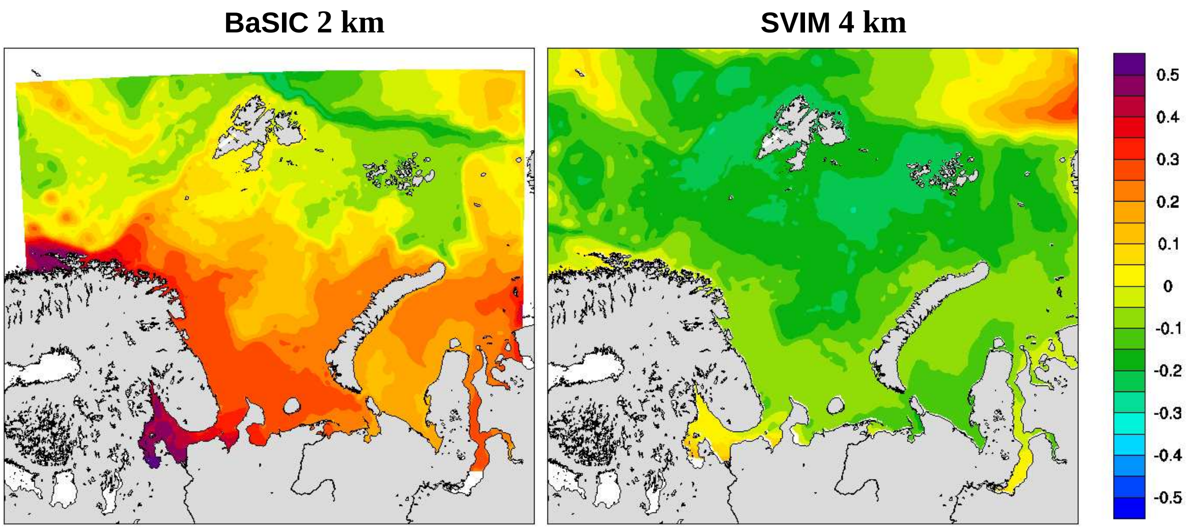


Figure 9: As Figure 6, but for the sea surface height (SSH). Color scale indicate the sea level in meters with a contour interval of 0.05 m for the range ±0.5 m. to Note the pronounced differences in sea level in the shallow parts of the domain, in particular in the Lofoten-Vesterålen area.

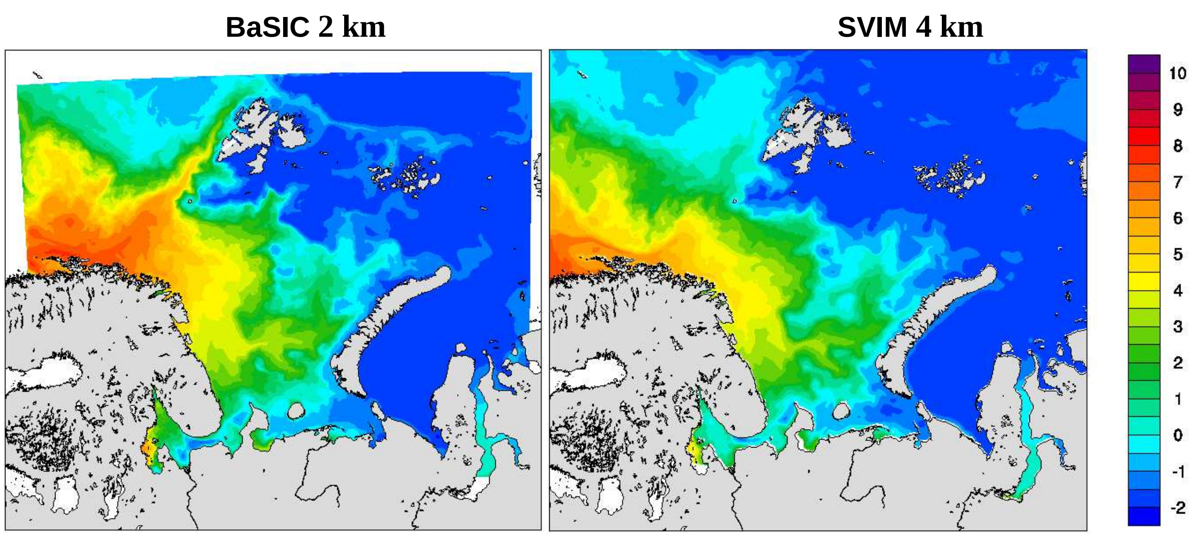


Figure 10: As Figure 6, but for the sea surface temperature (SST). Note the similarities in the patterns and that the BaSIC 2 km mesh model appears warmer along the coast and northward towards Spitsbergen.

the White Sea. They are present in both the SVIM 4 km mesh model as well as the BaSIC 2 km mesh model, but curiously enhanced in the BaSIC 2 km mesh model. One reason for the overall SSS discrepancies may be a weak SSS nudging applied in the SVIM 4 km mesh model. Another obvious reason for different SSSs in the to models is the lack of a proper sea ice input along the open boundaries of the BaSIC 2 km mesh model (Fig. 6. The consequence is less ice to melt once the initial ice is gone. Hence the freshwater fluxes become very different in

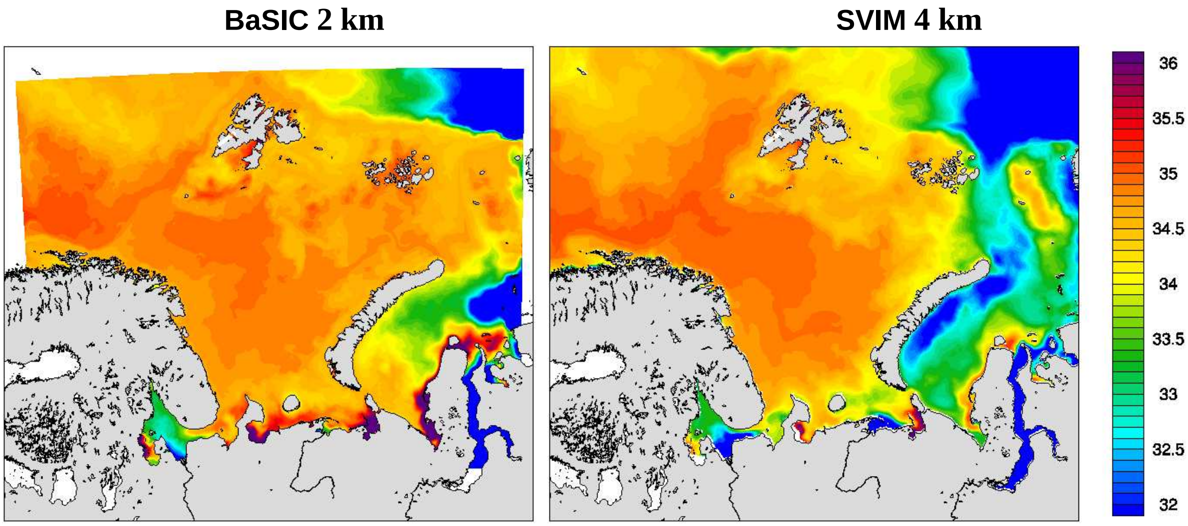


Figure 11: As Figure 6, but for the sea surface salinity (SSS). Note the differences along the Russian coast from the White Sea and into the Kara Sea. Color scale indicate salinity in intervals of 0.01 psu in the range 32 to 36 psu.

the two models, and may be an explanation for the overall higher SSS values in the BaSIC 2 km mesh model compared to the SVIM 4 km mesh model. Other obvious differences in the SSS is the tightening of the structures due to higher grid resolution.

# 5 Conclusions and recommendations

Described is the version of the triply nested model system that we are presently developing as part of the BaSIC (Barents Sea Ice and Currents) project as of February 21, 2013. Besides describing the technical set-up of the system we also discuss some results from test hindcasts.

The system consists of three models nested into each other. The outermost one, or the grandparent model, is the SVIM 4 km mesh model. The second, or parent model, is the BaSIC 2 km mesh model. The third and final, or child model, is the ultrafine BaSIC 800 m mesh model (Fig. 3).

We have run a 150 day test hindcast with the present system starting January 1, 2000. Results in terms of 30 day means covering the last 30 days of the hincast, that is, the period April 29 through May 28, 2000 are briefly discussed. Comparisons of results from the BaSIC 2 km mesh model and the SVIM 4 km mesh model show that

- More work is needed with regard to the lateral open boundary conditions (one-way nesting conditions),
    1. Lateral sea ice input must be included in the nesting conditions at the lateral open boundaries of the BaSIC 2 km mesh and the BaSIC 800 m mesh models (already remedied)

2. Rim currents should be minimized using the method described by *Mason et al.* (2010)

- Consider using sea surface salinity nudging also in the BaSIC 2 km mesh model and the BaSIC 800 m mesh model
- Consider using nudging of the sea ice concentration towards observed satellite based concentrations
- Consider enlarging the computational domain of the BaSIC 2 km mesh model to include the whole of the Lofoten Basin.

## Acknowledgment

This research was supported by Statoil Petroleum AS, Contract No. 4502465983, the Institute of Marine Research, Norway and the Norwegian Meteorological Institute. The computations were performed at the Norwegian Supercomputer facilities (the computer Vilje).

# References

Albretsen, J., A. K. Sperrevik, A. Staalstrøm, A. D. Sandvik, F. Vikebø, and L. C. Asplin (2011), Norkyst-800 Report No. 1: User manual and technical descriptions, *Tech. Rep. Fisken og Havet 2/2011*, Institute of Marine Research, Pb. 1870 Nordnes, N-5817 Bergen, Norway.

Dee, D. P., S. M. Uppala, A. J. Simmons, P. Berrisford, P. Poli, S. Kobayashi, U. Andrae, M. A. Balmaseda, G. Balsamo, P. Bauer, P. Bechtold, A. C. M. Beljaars, L. van de Berg, J.-R. Bidlot, N. Bormann, C. Delsol, R. Dragani, M. Fuentes, A. J. Geer, L. Haimberger, S. B. Healy, H. Hersbach, E. V. Hólm, L. Isaksen, P. Kållberg, M. Köhler, M. Matricardi, A. P. McNally, B. M. Monge-Sanz, J.-J. Morcrette, B.-K. Park, C. Peubey, P. de Rosnay, C. Tavolato, J.-N. Théaut, and F. Vitart (2011), The era-interim reanalysis: configuration and performance of the data assimilation system, *Quarterly Journal of the Royal Meteorological Society*, *137*(656), 553–597, doi:10.1002/qj.828.

Gerritsen, H., and A. C. Bijlsma (1988), *Computer Modelling in Ocean Engineering*, chap. Modelling of tidal and wind driven flow: The Dutch Continental Shelf Model, p. 9 pp., Schrefler & Zienckiewicz, Rotterdam, Balkema.

Griffies, S. M. (2004), *Fundamentals of ocean climate models*, Princeton University Press, ISBN 0-691-11892-2.

Haidvogel, D. B., H. Arango, P. W. Budgell, B. D. Cornuelle, E. Curchitser, E. D. Lorenzo, K. Fennel, W. R. Geyer, A. J. Hermann, L. Lanerolle, J. Levin, J. C. McWilliams, A. J. Miller, A. M. Moore, T. M. Powell, A. F. Shchepetkin, C. R. Sherwood, R. P. Signell, J. C. Warner, and J. Wilkin (2008), Ocean forecasting in terrain-following coordinates: Formulation and skill assessment of the regional ocean modeling system, *J. Comput. Phys.*, *227*(7), 3595–3624, doi:http://dx.doi.org/10.1016/j.jcp.2007.06.016.

Köhl, A. (2007), Generation and stability of a quasi-permanent vortex in the Lofoten Basin, *J. Phys. Oceanogr.*, *37*, 2637–2651, doi:10.1175/2007/JPO3694.1.

Koszalka, I. M., and J. H. LaCasce (2010), Lagrangian analysis by clustering, *Ocean Dyn.*, *60*, 957–972, doi:10.1007/s10236-010-0306-2.

Koszalka, I. M., J. H. LaCasce, M. Andersson, K. A. Orvik, and C. Mauritzen (2011), Surface circulation in the Nordic Seas from clustered drifters, *Deep Sea Res. I*, *58(4)*, 468–485, doi:10.1016/j.dsr.2011.01.007.

Kvingedal, B. (2005), Sea-ice extent and variability in the Nordic Seas, 1967-2002, in *The Nordic Seas: An Integrated Perspective*, *Geophysical Monograph Series Vol. 158*, edited by H. Drange, T. Dokken, T. Furevik, R. Gerdes, and W. Berger, American Geophysical Union, Washington, DC.

Marchesiello, P., J. C. McWilliams, and A. F. Shchepetkin (2001), Open boundary conditions for long-term integration of regional ocean models, *Ocean Mod.*, *3*, 1–20.

Mason, E., J. Molemaker, A. F. Shchepetkin, F. Colas, and J. McWilliams (2010), Procedures for offline grid nesting in regional ocean models, *Ocean Mod.*, *35*, 1–15, doi: 10.1016/j.ocemod.2010.05.007.

Reistad, M., Ø. Breivik, H. Haakenstad, O. J. Aarnes, and B. R. Furevik (2009), A high-resolution hindcast of wind and waves for the North Sea, the Norwegian Sea and the Barents Sea, *met.no Report 14/2009*, Norwegian Meteorological Institute, Postboks 43 Blindern, N-0313 Oslo, Norway.

Reistad, M., Ø. Breivik, H. Haakenstad, O. J. Aarnes, B. Furevik, and J.-R. Bidlot (2011), A high-resolution hindcast of wind and waves for the north sea, the norwegian sea, and the barents sea, *J. Geophys. Res.*, *116*(C5), n/a–n/a, doi:10.1029/2010JC006402.

Røed, L. P., and J. Debernard (2004), Description of an integrated flux and sea-ice model suitable for coupling to an ocean and atmosphere model, *met.no Report 4/2004*, Norwegian Meteorological Institute, P.O. Box 43 Blindern, 0313 Oslo, Norway, [Available at http://met.no/Forskning/Publikasjoner/Publikasjoner_2004/].

Røed, L. P., and N. M. Kristensen (2010), LOVECUR Final Report: Description of model and discussion of the model results, *met.no Report 21/2010*, Norwegian Meteorological Institute, P.O. Box 43 Blindern, 0313 Oslo, Norway, [Available at http://met.no/Forskning/Publikasjoner/Publikasjoner_2010/].

Røed, L. P., and N. M. Kristensen (2013), Eddy generation and cross shelf mixing off Lofoten, Norway, *Manuscript in preparation*.

Shchepetkin, A. F., and J. C. McWilliams (1998), Quasi-monotone advection schemes based on explicit locally adaptive dissipation, *Mon. Wea. Rev.*, *126*, 1541–1580.

Shchepetkin, A. F., and J. C. McWilliams (2005), The Regional Ocean Modeling System (ROMS): A split-explicit, free-surface, topography-following coordinate ocean model, *Ocean Modelling*, *9*, 347–404.

Shchepetkin, A. F., and J. C. McWilliams (2009), Correction and commentary for ”Ocean forecasting in terrain-following coordinates: Formulation and skill assessment of the regional ocean modeling system” by Haidvogel et al., J. Comp. Phys. 227, pp. 3595-3624, *J. Comp. Phys.*, *228*(24), 8985 – 9000, doi:10.1016/j.jcp.2009.09.002.

Song, T., and D. Haidvogel (1994), A semi-implicit ocean circulation model using a generalized topography-following coordinate system, *J. Comput. Phys.*, *115*, 228–244.

Umlauf, L., and H. Burchard (2003), A generic length-scale equation for geophysical turbulence models, *J. Marine Res.*, *61*, 235–265.

Warner, J. C., C. Sherwood, H. Arango, and R. Signell (2005), Performance of four turbulence closure methods implemented using a generic length scale method, *Ocean Modelling*, *8*, 81–113.